Land Use Policy 91 (2020) 104382

Contents lists available at ScienceDirect

Land Use Policy

journal homepage: www.elsevier.com/locate/landusepol

Local biophysical effects of land use and land cover change: towards an assessment tool for policy makers

Gregory Duveiller[a,*], Luca Caporaso[b], Raul Abad-Viñas[a], Lucia Perugini[b], Giacomo Grassi[a], Almut Arneth[c], Alessandro Cescatti[a]

[a] European Commission, Joint Research Centre (JRC), Ispra, VA, Italy
[b] Centro Euro-Mediterraneo sui Cambiamenti Climatici (CMCC), Viterbo, Italy
[c] Karlruher Institute fur Tecnologie (KIT), Garmish-Partenkirshen, Germany

ARTICLE INFO

Keywords:
LULCC
Biophysical effects
temperature
land-based climate policies

ABSTRACT

Land use and land cover change (LULCC) affects the climate through both biogeochemical (BGC) and biophysical (BPH) mechanisms. While BGC effects are assessed at global scale and are at the heart of climate treaties such as the Paris Agreement, BPH effects are totally absent despite their increasingly recognized impact, especially at local scale. This stems from the complexity in characterizing their climate impacts both at local and global scale, which makes it impractical to offer clear advices for the development of climate policies. To overcome this barrier, we built a prototype for an assessment tool to evaluate the local BPH impact of a series of land cover transitions. It relies on a dedicated methodology, based on satellite remote sensing data, that can estimate the local change in near surface air temperature associated with BPH effects of potential LULCC. This tool follows a tiered methodological approach, using transparent methods and mirroring what is currently provided by the IPCC to estimate the BGC effects, i.e. through different levels of increasing methodological complexity, from Tier 1 (i.e. default method and factors) to Tier 2 (i.e. similar to Tier 1 but with higher level of details and complexity) and Tier 3 (i.e. tailored solution to address national circumstances). The prototype tool enables the evaluation of the local impacts of land-related BPH effects, therefore facilitating a scientifically informed and comprehensive assessment of land-based climate policies.

1. Introduction

Land use and land cover change (LULCC) alters the climate by disrupting land-atmosphere fluxes of carbon, water and energy. A well-known process by which this occurs is defined as the biogeochemical (BGC) effect and depends on modifications in the net budget of greenhouse gases (GHG), such as CO_2 from changes in vegetation and soil organic carbon stocks, and CH_4 and N_2O in response mainly to crop, pasture and wetland management. The other main land-driven processes impacting climate depends on variations of the surface energy budget mediated by albedo, evapotranspiration and roughness (biophysical BPH effects) (Pielke et al., 1998; Betts, 2000; Bonan, 2008; Lee et al., 2011; Anderson-Teixeira et al., 2012; Mahmood et al., 2014; Zhang et al., 2014; Li et al., 2015; Alkama and Cescatti, 2016; Duveiller et al., 2018c).

To illustrate the differences between BGC and BPH climate effects of LULCC, we can consider a generic conversion from forest to cropland. From the biogeochemical perspective, this would contribute to global warming by releasing part of the carbon stock in the forest, in a form and time that depends on the modality and scope of conversion (e.g. burning for land clearing vs. use of wood for specific purposes), but also by diminishing the carbon capture capacity of the ecosystem. From the biophysical side, this deforestation process typically entails a rapid increase in albedo and a concomitant decrease in evapotranspiration that may ultimately lead to either a local cooling or a local warming effect (Perugini et al., 2017), depending on which of the two processes dominates (Davin and de Noblet-Ducoudré, 2010; Bright et al., 2017), depending on the size and pattern of the LULCC perturbation (Pitman and Lorenz, 2016), and depending on the background climate (Pitman et al., 2011; Huang et al., 2018). BGC and BPH also differ in how fast and how far their effects are felt. There will necessarily be some latency between the moment when more net carbon is added to the atmosphere as a consequence of local deforestation and its global greenhouse effect, while the biophysical changes in albedo and evapotranspiration, and thus temperature, are almost immediate. Analogously, the BGC effects of local deforestation will be felt globally, while those of BPH will

* Corresponding author.
E-mail address: gregory.duveiller@ec.europa.eu (G. Duveiller).

https://doi.org/10.1016/j.landusepol.2019.104382
Received 2 August 2018; Received in revised form 12 November 2019; Accepted 24 November 2019
Available online 04 December 2019

generally be concentrated on where it happened. However, LULCC can also have non-local BPH effects due to changes in wide-ranging climate circulation (Winckler et al., 2017), which is when LULCC at some place affects the climate elsewhere via atmosphere or ocean teleconnections. Finally, the BPH effects can be both direct and indirect (Devaraju et al., 2018). An example of an indirect effect is how a decrease in evapotranspiration due to deforestation also changes the cloud regime, thereby indirectly changing the incoming solar radiation.

To complicate matters, local BPH effects can act on top of ongoing BGC climate effects to potentially exacerbate their impact and be highly relevant for land use policy. This can occur despite the fact that local BPH effects become negligible when averaged globally (as local warming can be compensated by local cooling elsewhere), because locally they can magnify or dampen warming impacts due to BGC depending on the location and type of LULCC (e.g. Huang et al., 2018). As an example, let us consider the case of crop production. Climate change is expected to expand cropland suitability in the Northern Hemisphere high latitudes, while the tropics will experience a contraction of cropland suitability (Ramankutty et al., 2002). A recent study (Zhao et al., 2017) further reports that, without CO_2 fertilization, raising temperatures have consistently negative impacts on the yields of four major crops (wheat, rice, maize, soybean) at the global scale, undermining food security. From the BPH side, observations show a consistent regionally-averaged local cooling of 0.6 °C on average in boreal areas due to deforestation, with results ranging between -0.95 to +0.04 °C and a warming of the same amplitude for deforestation in tropical area (0.41 ± 0.57 °C) (Perugini et al., 2017; Alkama and Cescatti, 2016; Zhang et al., 2014; Lee et al., 2011). These immediate BPH effects of LULCC alter the local ecosystem energy balance and could have further impacts on crop distribution and production, possibly affecting food supply in the long term. Understanding the environmental impacts of land policies in a comprehensive way, including the temperature changes due to BPH effects, can be of high importance for policy makers to ensure proper land planning.

How can BGC and BPH effects be evaluated and monitored? The answer depends on the effect. Global BGC effects can be inferred from national GHG inventories and book-keeping techniques (Houghton and Nassikas, 2017). Modelling, whether statistically-based extensions of forest inventory data, such as the Carbon Budget Model (Kurz et al., 2009), or mechanistic process-based models such as dynamic global vegetation models (DGVMs) used in Earth System Models (ESMs), can provide valuable feedback for evaluating carbon stocks and fluxes (Le Quéré et al., 2018). Satellite remote sensing techniques could be very valuable due to their synoptic coverage, but measuring carbon fluxes and stocks directly from space is notoriously difficult (e.g. Stocker et al., 2019). On the other hand, the complete BPH effect, including both direct and indirect components as well as both local and non-local aspects, can only be quantified using land-atmosphere climate models. Yet these models still show considerable uncertainties when analyzing LULCC, specifically regarding the characterization of changes in non-radiative fluxes (de Noblet-Ducoudré et al., 2012). More critically, the computational complexity in running such coupled models makes it currently unfeasible to provide policy-advice at the relevant local scale at which LULCC occur and for all parts of the world. While recent studies have been able to focus on finer representations of LULCC (e.g. Winckler et al., 2017; Quesada et al., 2017), what is considered a local change is still at the scale of an entire climate model grid cell (typically $\geq$ 10000 km^2). Satellite remote sensing can provide a much finer estimate ($\leq$ 5 km^2) of local BPH effects (Zhang et al., 2014; Li et al., 2015; Alkama and Cescatti, 2016; Duveiller et al., 2018c), which have recently revealed further the discrepancies amongst models to capture such local BPH effects at this scale (Duveiller et al., 2018a). However, these remote sensing techniques can currently only provide the local effects, and not the non-local effects (i.e. teleconnection).

There is also a stark contrast between how BGC and BPH effects are considered in climate policies for land-based mitigation and adaptation. The Paris Agreement (PA) long-term goals include holding "the increase in the global average temperature to well below 2°C" (Article 2). To this aim, countries that ratified the PA are expected to communicate and periodically update nationally determined contributions, i.e. their pledges to reduce the greenhouse gases emissions (GHG) regulated under the United Nations Framework Convention on Climate Change (UNFCCC). The UNFCCC and its PA, in other words, implicitly assume that reducing GHG (i.e. BGC effects) is the only way through which countries may mitigate climate change. A high expectation for forest mitigation emerges both in countries' climate targets (i.e., the Nationally Determined Contributions, NDCs), where forests are assumed to provide up to a quarter of planned emission reductions by 2030 (Grassi et al., 2017), and in estimates of land-based mitigation potential (Griscom et al., 2017) and pathways to achieve the 2°C target (Rockström et al., 2017). However, forest and land based solutions for climate mitigation and adaptation goals extend beyond the carbon cycle (Ellison et al., 2017; Seneviratne et al., 2018).

The fact that BPH effects are still ignored by climate policies contributes to an incomplete evaluation of the climate impacts of anthropogenic LULCC. The reasons for such omission are primarily related to the high level of complexity associated with quantifying the BPH impacts, which has made it impractical to offer clear advice on the most-effective policy and on which level policy makers can act (Perugini et al., 2017). The combination of BPH and BGC effects at both local and/or global levels would be advisable for the comprehensive assessment of climate policies, but it is yet unclear how to compare the two climate effects together. Several studies have already advocated a more complete evaluation of the net climate effect of LULCC policies on climate, beyond the global warming potential (Pielke et al., 2002; Marland, 2003; West et al., 2011; Gotangco Castillo et al., 2012), but without providing any metric or composite index. While some metrics have been proposed (Bright, 2015), they have not yet been adopted at large scale due to complexity of monitoring them at the appropriate spatial and temporal scales. The process of including land-based mitigation in the UNFCCC context has been a matter of long and complex negotiations (UNFCCC, 2011b,a; United Nations, 2015; Grassi et al., 2018). While adding the land-related BPH effects to the scope of country reporting under UNFCCC (currently entirely focused on GHG) would currently be very difficult from the political perspective, the availability of concrete tools to assess the impacts of BPH effects (mainly at local level) would facilitate a better informed and science-based land planning by policy makers.

The objective of this study is to provide a prototype for an assessment tool that can be used by policy makers to quantify the local biophysical impacts of LULCC. This impact is summarized by the expected change in annual near surface air temperature over a given area following a specific LULCC transition occurring over the same area. The tool follows a tiered methodological approach mirroring what is currently provided by the IPCC to estimate the biogeochemical effects (IPCC, 2006), i.e. through different levels (Tiers) of increasing methodological complexity, from Tier 1 (i.e. default method and factors) to Tier 2 (i.e. higher level of complexity) and Tier 3 (i.e. tailored solution to address national circumstances with finer granularity in both spatial and temporal resolutions). Here, we generate and analyse the numbers for Tier 1 and 2 based on satellite remote sensing observations, and we discuss a blueprint on how the same methodology can be applied to provide national solutions using dedicated data layers for a Tier 3 approach. All the numerical values behind the tool are available in the supplementary section of this study.

2. Material and Methods

2.1. Retrieval of the local temperature change

The tool requires estimates of how local air temperature rises or falls following a given land cover change. To obtain these numbers we apply

Table 1
IPCC LC classes and their descriptions (IPCC 2006, Vol: 4, Ch: 3; Page 3.6 in: http://www.ipcc-nggip.iges.or.jp/public/2006gl/vol4.htmlhttp://www.ipcc-nggip.iges.or.jp/public/2006gl/vol4.html).

IPCC Land Use categories	Description
(i) Forest Land	This category includes all land with woody vegetation consistent with thresholds used to define Forest Land in the national greenhouse gas inventory. It also includes systems with a vegetation structure that currently fall below, but in situ could potentially reach the threshold values used by a country to define the Forest Land category.
(ii) Cropland	This category includes cropped land, including rice fields, and agro-forestry systems where the vegetation structure falls below the thresholds used for the Forest Land category.
(iii) Grassland	This category includes rangelands and pasture land that are not considered Cropland. It also includes systems with woody vegetation and other non-grass vegetation such as herbs and shrubs that fall below the threshold values used in the Forest Land category. The category also includes all grassland from wild lands to recreational areas as well as agricultural and silvo-pastoral systems, consistent with national definitions.
(iv) Wetlands	This category includes areas of peat extraction and land that is covered or saturated by water for all or part of the year (*e.g.* peatlands) and that does not fall into the Forest Land, Cropland, Grassland or Settlements categories. It includes reservoirs as a managed sub- division and natural rivers and lakes as unmanaged sub-divisions.
(v) Settlements	This category includes all developed land, including transport infrastructures and human settlements of any size, unless they are already included under other categories. This should be consistent with national definitions.
(vi) Other Land	This category includes bare soil, rock, ice, and all land areas that do not fall into any of the other five categories. It allows the total of identified land areas to match the national area, where data are available. If data are available, countries are encouraged to classify unmanaged lands by the above land use categories (*e.g.* into Unmanaged Forest Land, Unmanaged Grassland, and Unmanaged Wetlands). This will improve transparency and enhance the ability to track land use conversions from specific types of unmanaged lands into the categories above.

a tested methodology (Duveiller et al., 2018c) to a new dataset of satellite-derived monthly air-surface temperature data (Hooker et al., 2018). The methodology relies on comparing values of temperature over neighbouring areas with similar environmental conditions but contrasting land cover types, an approach that has also been adopted by several other studies (e.g. Zhao and Jackson, 2014; Li et al., 2015; Peng et al., 2014). The assumption is that the temperature measured over a given land cover type, e.g. a grassland, is a valid estimation of the temperature that a different land cover type in the vicinity, e.g. a forest, would have if the latter was converted to the former (i.e. the result of replacing a forest by a grassland). An advantage of this approach is that estimations of temperature change can be made even when actual LULCC has not occurred. Because this local temperature change strongly varies both spatially and seasonally and depends on the background climate (Pitman et al., 2011), it is difficult to rely on ground measurements, which would typically not allow sufficient spatial coverage to be representative for all areas across the world. However, current satellite Earth observation offers the capacity to sample the globe systematically and consistently: an ideal technology for this kind of application.

There is a difference between the radiant land surface temperature (LST) that can be estimated directly from remote sensing and the air temperature considered in climate policy. The latter is referred to here as T_{2m}, and is defined as the near-surface air temperature measured in a weather station under standard conditions, which means in a white box 2 m above a trimmed grass canopy cover WMO (1996a,b). For the sake of brevity, from henceforth in this text we refer to this near-surface air temperature simply as air temperature or as T_{2m}. T_{2m} also differs from the LST retrieved from satellite in that the former does not have a clear-sky bias. Under overcast conditions, the satellites used to generate the LST cannot sample the surface below the clouds, generating a bias for clear-sky days.

Since the relationship between LST and T_{2m} is not constant in space and time, Hooker et al. (2018) established a dedicated regression procedure leveraging on both geographic and climatic similarity criteria to relate LST from the MODIS AQUA platform to monthly temperatures derived from station data from the Global Historical Climatology Network-Monthly or GHCN-M (Lawrimore et al., 2011). These regressions were then applied to the exhaustive coverage of satellite LST to generate a T_{2m} dataset providing values for all places where station data are not available. This approach has the added benefit of removing the clear-sky bias inherent in the LST data. Research has shown that LST and T_{2m} do respond slightly differently to LULCC processes such as deforestation (Winckler et al., 2018), but this has been neglected in the present study as the Hooker et al. (2018) dataset does not employ any information of land cover explicitly when converting LST to T_{2m}. The pixel-wise monthly-median values of this T_{2m} dataset are calculated over the period 2008-2012 and used in combination with the ESA climate change initiative land cover map for 2010 (ESA, 2017) to generate maps of local temperature changes following the methodology described in Duveiller et al. (2018c). These temperature changes are aggregated to a spatial resolution of $1^\circ \times 1^\circ$ and averaged annually (from their original monthly temporal resolution) for each considered land use transition. In parallel, the same temporal aggregation is applied to the original LST datasets provided by Duveiller et al. (2018b) to produce the same information for three variables: T_{2m}, LST_{day} and LST_{night}.

2.2. Harmonization of land use classes

The study of Duveiller et al. (2018c) targeted vegetation cover change and relied on the land cover classes of the ESA maps to define the vegetation transitions that could be analysed. The resulting classes are based on the global vegetation classification scheme of the International Geosphere Biosphere Programme (IGBP). The same approach is used here, but we aim to harmonize these vegetation classes with the classes of land use defined by the IPCC and used in the assessment framework for BGC effects (see Table 1). All different forest types in the IGBP scheme, namely evergreen broadleaf forests (EBF), deciduous broadleaf forests (DBF), evergreen needleleaf forests (ENF), deciduous needleleaf forests (DNF) and mixed forest (MD), are gathered together to represent the Forest land class in the IPCC nomenclature (IPCC, 2006). IGBP classes of savannas (SAV), shrublands (SHR), grasslands (GRA) are grouped into the general Grassland definition of IPCC, which tolerates isolated trees and shrubs. Forest land and Grassland are complemented by Croplands and Wetlands, both directly remapped from the respective cropland (CRO) and wetlands (WET) classes in the IGBP scheme, to make up the 4 land uses classes considered here for Tier 1. However, for Tier 2 all possible transitions amongst the IGBP classes are considered. Table 2 summarizes the correspondence between the IPCC and IGBP classes.

2.3. Spatial gap-filling

While the space for time substitution behind the methodology of Duveiller et al. (2018c) is capable of providing information on temperature change in the absence of actual LULCC, it still requires a certain level of co-occurrence of both land use types within a local vicinity. In areas where a given land use type does not currently exists, no information is available regarding its possible introduction, for instance precluding the use of the tool to assess impacts of afforestation

Table 2
Summary of the correspondences between IPCC Land Use Categories System and the land cover categories at Tier 1 and Tier 2 level used in this study

IPCC Land Use Categories	Tier 1 Level	Tier 2 Level
Forest Land	Forest Land	Evergreen Broadleaf Forest (EBF) Decidous Broadleaf Forest (DBF) Evergreen Needle-leaf Forest (ENF) Decidous Needle-leaf Forest (DNF) Mix Forest (MF)
Grassland	Grassland	Savannah (SAV) Shrubland (SHR) Grassland (GRA)
Cropland	Cropland	Cropland (CRO)
Wetland	Wetland	Wetland (WET)

programs where there is currently no comparable forest. To mitigate this caveat, we adopt an extra post-processing step to fill-in the spatial gaps in the maps of local temperature change based on similarities in local climate. For this purpose, the monthly temperature and precipitation for the period 2008-2012 are compiled at $1^\circ \times 1^\circ$ spatial resolution from the CRU data version 4.00 (Harris et al., 2014). Based on these values, the following four climate indicators are calculated for each year: mean annual temperature (T), annual temperature range (temperature difference between coldest and warmest months), cumulated precipitation over the year (P) and aridity index for that year (defined as $P/(T + 30)$). The 5-year median values of these indicators are then used along with the values of local temperature change to train a machine learning algorithm to estimate the latter from the former. The trained algorithm can thus be used to predict local temperature changes based on climate for areas where the original space for time method had insufficient samples to produce data.

The machine learning method used here is the random forest (Breiman, 2001; Ho, 1998), which consists in constructing a multitude of regression trees and select the mean prediction of the individual trees. We employ the `R` implementation within the `randomForest` package with the default settings of 500 individual trees. The gap-filling approach is applied to every annual temperature change map, i.e. for every individual transition between land classes of either Tier 1 or Tier 2, and for all three variables (T_{2m},LST_{day} and LST_{night}). However, precautions have been taken to ensure these predicted outputs remain realistic. First, we remove all areas from the predicted outputs in which neither of the two land use types involved in a given transition is present according to the ESA land cover distributions (we consider absence if the area covered within a $1^\circ \times 1^\circ$ grid cell is below 5%). In practice it is indeed possible to have a place with a climate that could potentially host the land covers involved in a transition, but that neither of them are actually present to a reasonable extent. Second, the random forest is only used in interpolation, i.e. only using combinations of climate indicator values that are actually observed for the transition in question. This ensures that we avoid situations in which a given land use type is assumed to be established in areas where the climatic conditions are not appropriate for the corresponding vegetation type. Finally, we noticed that the outputs of the random forest could have a clear systematic bias with respect to the magnitude of the signal, i.e. underestimating positive values and overestimating negative ones (not shown here). To correct for this effect, we applied a simple linear regression to ensure the output is scaled to the range of the original data. As an indication, the resulting root mean squared deviations with the original T_{2m} data after the entire procedure (machine learning plus bias correction) ranges between 0.17 °C and 0.19 °C for Tier 1 and between 0.13 °C and 0.33 °C for Tier 2.

2.4. Aggregation

The gap-filled maps of annual changes in local temperature due to LULCC need to be aggregated to a single value per transition and per climate zone. To do so, we use the climate zones shown in Fig. 1 , which are defined by the IPCC based on elevation, mean annual temperature, mean annual precipitation, frost occurrence, and the ratio between mean annual precipitation and potential evapo-transpiration (IPCC, 2006). The climate zones are provided in a finer grid of 1/12° cells, resulting in several climate zones attributed to each 1° grid cells of local temperature change data that straddles across climate zone boundaries. Therefore, when calculating a mean value for a given climate zone, mixed grid cells are only counted proportionally to the fraction of area within the larger 1° cell covered by the climate zone in question. To ensure that the estimated means remain robust, these are only calculated when a minimum amount of samples are available for a given transition within a specific climate zone. This minimum is set to 30 for Tier 1, while 15 samples are tolerated for Tier 2, where values are provided further divided in the sub-continental regions delimited in Fig. 1 .

Another precaution taken in this aggregation step is to filter out areas characterized by large local variations in topography from the climate zone map. The reason for doing this is that the local temperature changes only relate to flat areas (Duveiller et al., 2018c), since local differences in elevation would compromise the assumption of comparable conditions when replacing space for time. Using the same topographical masking rules described in detail in Duveiller et al. (2018b), we mask out climate zone pixels where more than half the area corresponds to unfavourable terrain prior to aggregation. These final aggregated values are provided in a single table in the supplementary material of this paper, containing the separate estimates for T_{2m}, LST_{day} and LST_{night}. This table is the basis of the prototype tool for policy-makers. While LST values are provided for the sake of completion, the following results will only be discussed in terms of T_{2m}. However, all plots presented here are also available for both LST_{day} and LST_{night} in the Supplementary Material of this paper.

3. Results

3.1. Tier 1: overview of global figures

The spatial patterns of the estimated mean annual changes in local air temperature due to the transitions of the four land use classes considered in Tier 1 are depicted in Figure 2 . The actual numbers we propose to use in the tool are the values in Figure 2 aggregated by climate zones, which are presented in Figure 3 . In both cases, transitions are considered amongst two land systems in equilibrium, making them symmetric, e.g. the change in temperature following a conversion from forestland to cropland is the same in magnitude than that of a conversion of cropland to forestland, but with an opposite sign. It should be stressed that this symmetry is not expected immediately after the perturbation generated by the land cover change, but only after a given time lag during which the landscapes have reached a new biophysical equilibrium.

Figure 2 shows how the impact of deforestation follows a general latitudinal gradient: a moderate local biophysical cooling effect due to the increase in surface albedo from snow cover in large areas of cool temperate and boreal regions and a clear warming effect due to both evapotranspiration efficiency and surface roughness decrease in most warm temperate and tropical regions. However, there can be stark differences according to water availability, as seen by the clear change in sign between dry and moist climates in North America. These patterns are generally comparable whether forests are replaced by either grasslands or croplands, but the warming effects seem more important for grasslands in dry areas (see Figure 3).

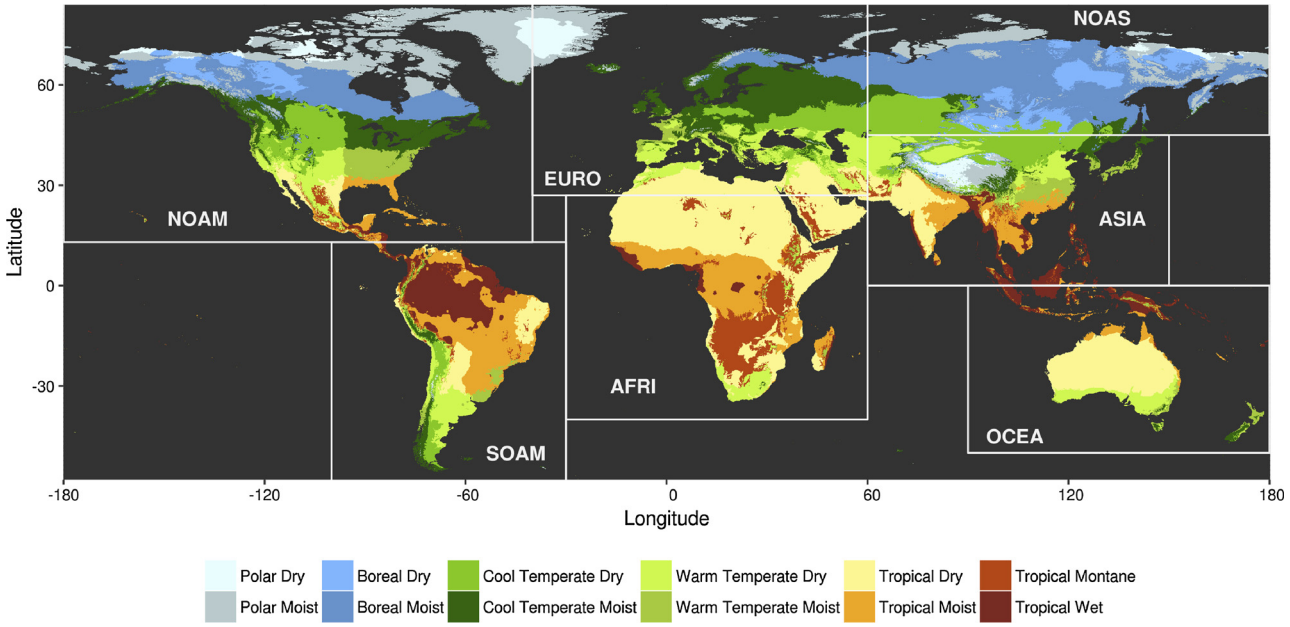

Fig. 1. Climate zones as defined by the IPCC and considered for aggregation in Tier 1 and Tier 2 of the proposed assessment tool. (IPCC 2006, Vol: 4, Ch: 3; Page 3.6 in: http://www.ipcc-nggip.iges.or.jp/public/2006gl/vol4.html). The delimited sub-continental regions are those used for the finer aggregation at Tier 2 level.

The conversion of grasslands to croplands leads to less pronounced changes in temperature that do not follow the same latitudinal logic as deforestation. Instead, these patterns might be more related to which crops are planted and how they are managed in different regions across the world. Irrigation in particular would favour a cooling of the surface due to the enhancement of surface evapotranspiration (Thiery et al., 2017). This may explain the considerable cooling observed in Figure 2 for the grassland to cropland conversion in places like North America, Australia, Central and South Asia, while in Europe, where there is less tendency to irrigate (Siebert et al., 2005), the trend is towards warming. Another factor to consider is that the Tier 1 definition of grasslands also includes shrublands and savannas, making a general interpretation of such patterns more complicated.

The third type of land use conversion that can be explored in Tier 1 is the replacement of wetlands by either forestland, cropland or grassland. The clearest patterns appear in the case of wetlands to forestland conversion, where there is a stark contrast between a mean annual cooling in tropical regions and a mean annual warming effect in boreal regions. Wetlands, whether composed of flooded forests or flooded low-vegetation ecosystems, typically have lower productivity than neighboring non-flooded forest, resulting in lower evaporative cooling. However, they also have shallower roots. As they generally do not stay flooded all year round, and they are exposed to a dry season during which these shallower roots have a more limited access to water, they evapotranspirate even less. In the case of tropical wetlands, this effect during the dry season dominates the annual signal. In the case of boreal wetlands, which generally consists only of non-forested ecosystems, this effect is instead counter-balanced by the strong snow albedo effect during winter and spring time. Snow over non-forested wetlands will reflect more energy back into space, while the trees emerging from the snow will absorb more radiation due to their darker surface, resulting in an annual signal of warming when considering the conversion of wetlands to forests.

3.2. Tier 2: increasing detail

Whereas Tier 1 provides global values with a simplified aggregation approach, Tier 2 offers more refinement both by focusing on the sub-continental scale and by providing more granularity in the land use transition typology that is considered (using 10 land classes instead of 4). The number of values for all transitions across climate zones and sub-continental regions rises up to 816, making it difficult to present them all synthetically in a meaningful figure. Therefore, the focus is here placed on illustrating the increase in detail obtained when comparing Tier 1 to Tier 2 for the selected cases of afforestation in Europe and the conversion from grassland to croplands in Asia. However, the numbers for all other cases are available in the supplementary material.

The case of afforestation in Europe and its neighbourhood is represented in Figure 4 . Afforestation is here understood as the Tier 1 transition from cropland to forestland following the IPCC land use class definition, which can be obtained by inverting the sign around the transition from forestland to cropland shown in Figure 2 . For each subplot corresponding to one of the major climate zones encountered in the area, the first bar provides as a reference the global temperature change value used in Tier 1 (T1). The second bar is an intermediate value (T1*) in which the general Tier 1 transition of cropland to forestland is averaged only over the considered sub-continental region, thus revealing geographic specificities. For example, with the exception of forests in cool temperate moist climates, forests in the other 4 main climate regions have a tendency to cool more or warm less in this extended European region than in the rest of the world (*i.e.* the T1* values are lower than the T1 values). The following bars depict how the number can vary according to the type of forest that is considered for afforestation. An example of different forest behaviour can be noted in the warm temperate dry climate where the decrease in temperature is higher when replacing DBF (which typically evapotranspirate more under this climate and thus cool more the land) than when planting ENF (which are generally darker, and thus warmer to begin with). There are also some more surprising behaviours, such as the strong cooling effect of planting EBF in cool temperate moist climate or the warming behaviour of establishing a DNF in cool temperate dry climate. However such plant types are atypical in these climates and these numbers might reflect a shortcoming in the gap-filling approach based on too few samples or sub-optimal climate predictor variables for these particular cases.

The second case featured in Figure 5 illustrates the Tier 2 refinement of the Tier 1 grasslands to croplands transition in the Asia sub-region. This conversion can be considered as an intensification of the anthropic influence on the landscape, as croplands would typically be managed more intensively than either savannas, shrublands or

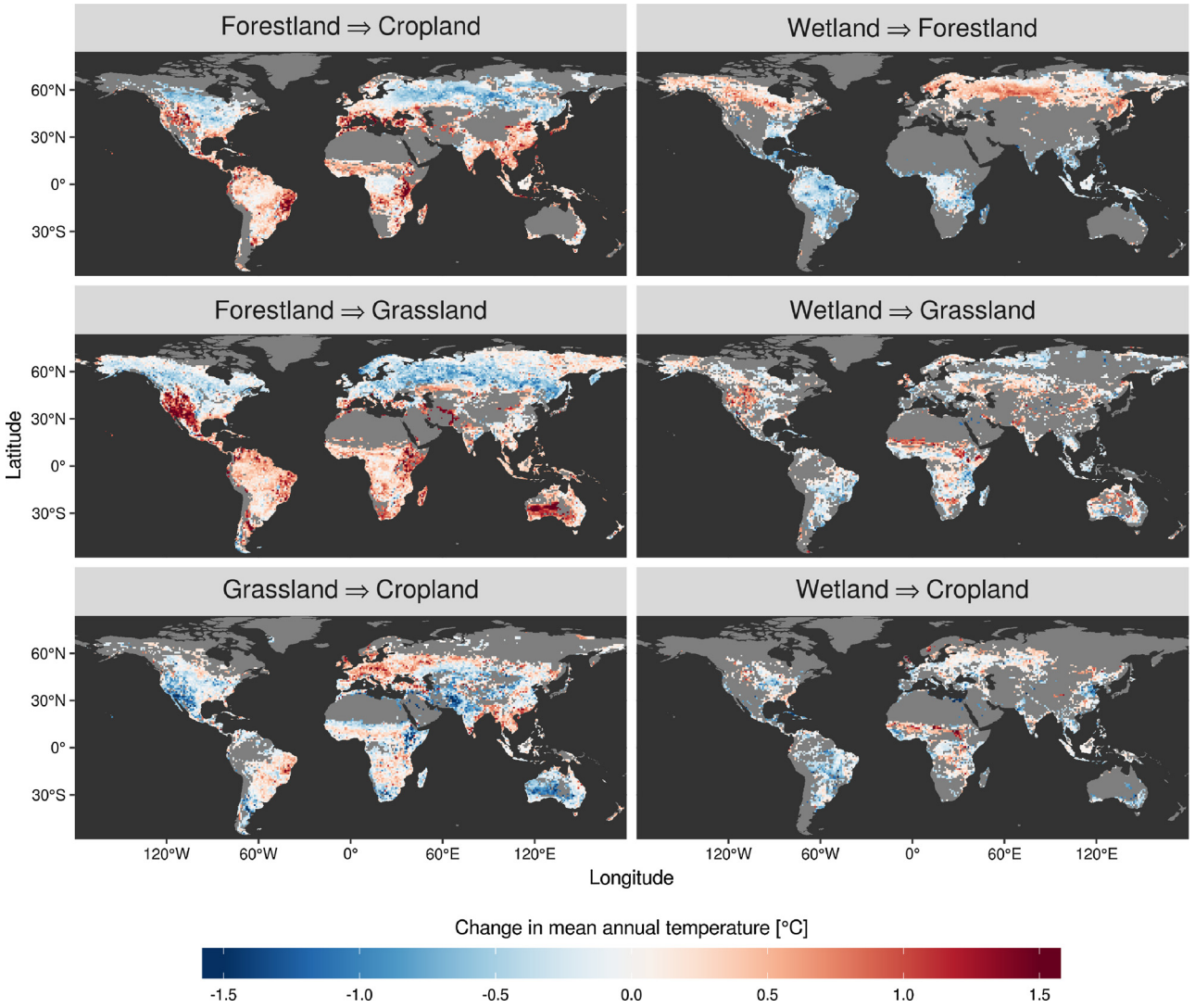

Fig. 2. Estimated values of mean annual temperature change as a cause of LULCC for different potential transitions at Tier 1 level. Grey areas indicate places where no estimations are available because both classes do not co-exist and no gap-filling was possible.

grasslands (the 3 components of the Tier 1 grassland class). Figure 5 illustrates how the refinement of the final land use classes can change the sign of the temperature change, *e.g.* in tropical wet or moist climate the result is cooling when grasslands are converted to croplands, but it turn to warming when the conversion targets more natural systems such as shrublands or savannas. The regionalization benefit of Tier 2 is visible for the polar climate of the Tibetan plateau, which is expected to behave differently to other places with polar climates due to its location at lower latitudes, exposing it to more solar radiation. Another example is in the tropical dry region in South-Asia, where a considerable part of croplands is under irrigation, which would cool more the land than when considering all tropical dry zones globally.

4. Discussion

The framework described above for both Tier 1 and Tier 2 of the proposed assessment tool not only serves as a proof-of-concept for the methodological approach, but it can also be directly used in practice to assess the local biophysical effects of LULCC. The numbers provided are a trade-off between detail and simplicity in that only a mean annual change in air temperature is provided per climate zone and (for Tier 2) per region. Further refinements could be adjusted by provided metrics informing on the resulting seasonal amplitude of temperature, analysing the effects of extreme events, or increasing the spatial granularity to represent individual countries. However, to respect the logic of the BGC framework with a 3-tiered approach, the increase in complexity and detail should be reserved to the tool's Tier 3.

The construction of Tier 3 can be methodologically identical to that of Tiers 1 and 2. Since the space-for-time substitution approach is not dependent on scale (Duveiller et al., 2018c), both in terms of the spatial resolution of the input data and the thematic detail of the input classifications, it can readily be applied at finer levels. Tier 3 could therefore consist of applying the method at country or region level, possibly using finer spatial resolution remote sensing data if it becomes available. However the real added-value would be the use of local thematic maps, which would both have a higher accuracy than the global land cover maps and which can focus on land use, and thus management, rather than only on land cover. This opens the possibility of tailored solutions to tackle the different landscapes across the world, exploring the effects of differences in forest structure, in crop types or in management practices (irrigation, zero-tillage). Regional examples could include exploring the effect of shade in cocoa agro-forestry plantations in West Africa (Abdulai et al., 2018) or using forest-structure classifications in Fennoscandia (Majasalmi et al., 2017).

Since no Tier 3 implementation is currently available, some further discussion is warranted on the use Tier 1 and Tier 2. Despite the efforts

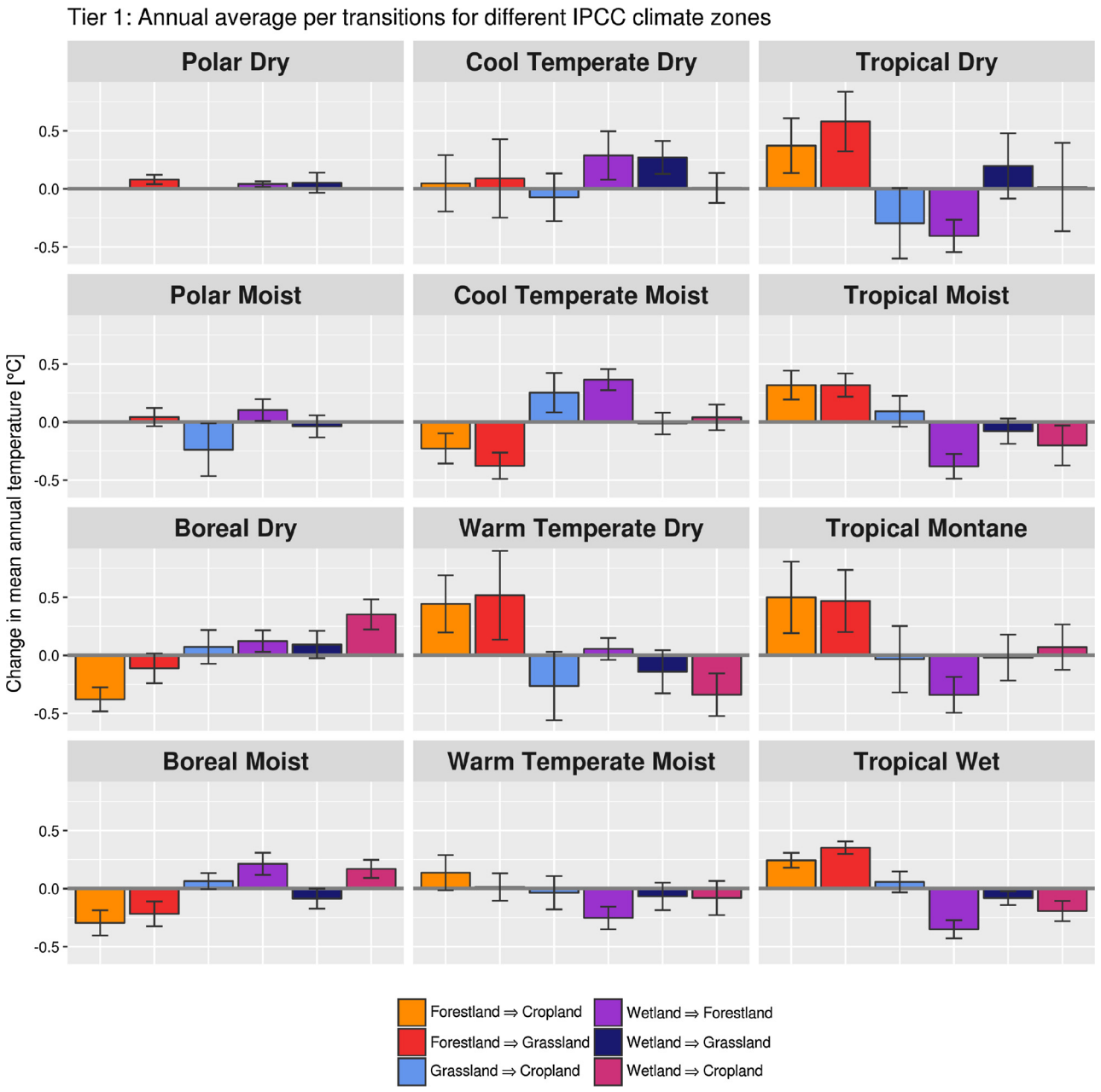

Fig. 3. Bar charts showing the changes in mean temperature following potential transitions aggregated per climate zones at Tier 1 level. The error bars show the spatial variability around the means and correspond to ± 2 standard deviations of the population of all values for a given transition in a given climate.

to match the present classes with the IPCC categories, caution should be taken in the interpretation since some inconsistencies may arise given that the former refer strictly to land cover characteristics while in the latter the land use often dominates over land cover. For example, cropland currently covered by grasses as fallow, as part of the crop rotation cycle, is usually classified as cropland in the IPCC reporting, while it should be considered as grassland in the present tool, since the biophysical effect is linked with the type of cover currently present on site. In other cases, land management could strongly affect biophysical exchange between land and atmosphere, as in the cases of irrigated cropland vs. rain-fed where the presence of water will strongly affects the local energy balance and thus the local climate. Another point is that the current version of the tool does not include transitions involving the IPCC classes of "Settlements" and "Other lands" because the original approach (Duveiller et al., 2018c) focused only on vegetated classes. Furthermore, the surface to air temperature conversion (Hooker et al., 2018) was not optimized for urban environments where differences between surface and air temperature are much larger than over vegetated areas. A further refinement of the tool could target urban dynamics using a dedicated input layer such as the global human settlement layer (Pesaresi et al., 2016), but may require a dedicated source of gridded near-surface air temperature for urban environments.

There are also other considerations beyond the classification concepts that must be understood when using the tool to quantify the local BPH effects of LULCC. First, the changes of temperature only relate to the area where LULCC has occurred. The increase in temperature reported following tropical deforestation is only going be felt locally, unlike the biogeochemical repercussions which typically get averaged in the atmosphere. However, these biophysical increases in temperature may be more pertinent for local/regional policy-making as it is the one that will be immediately affecting the people living there. In the same vein, we re-iterate that non-local BPH effects of the potential LULCC

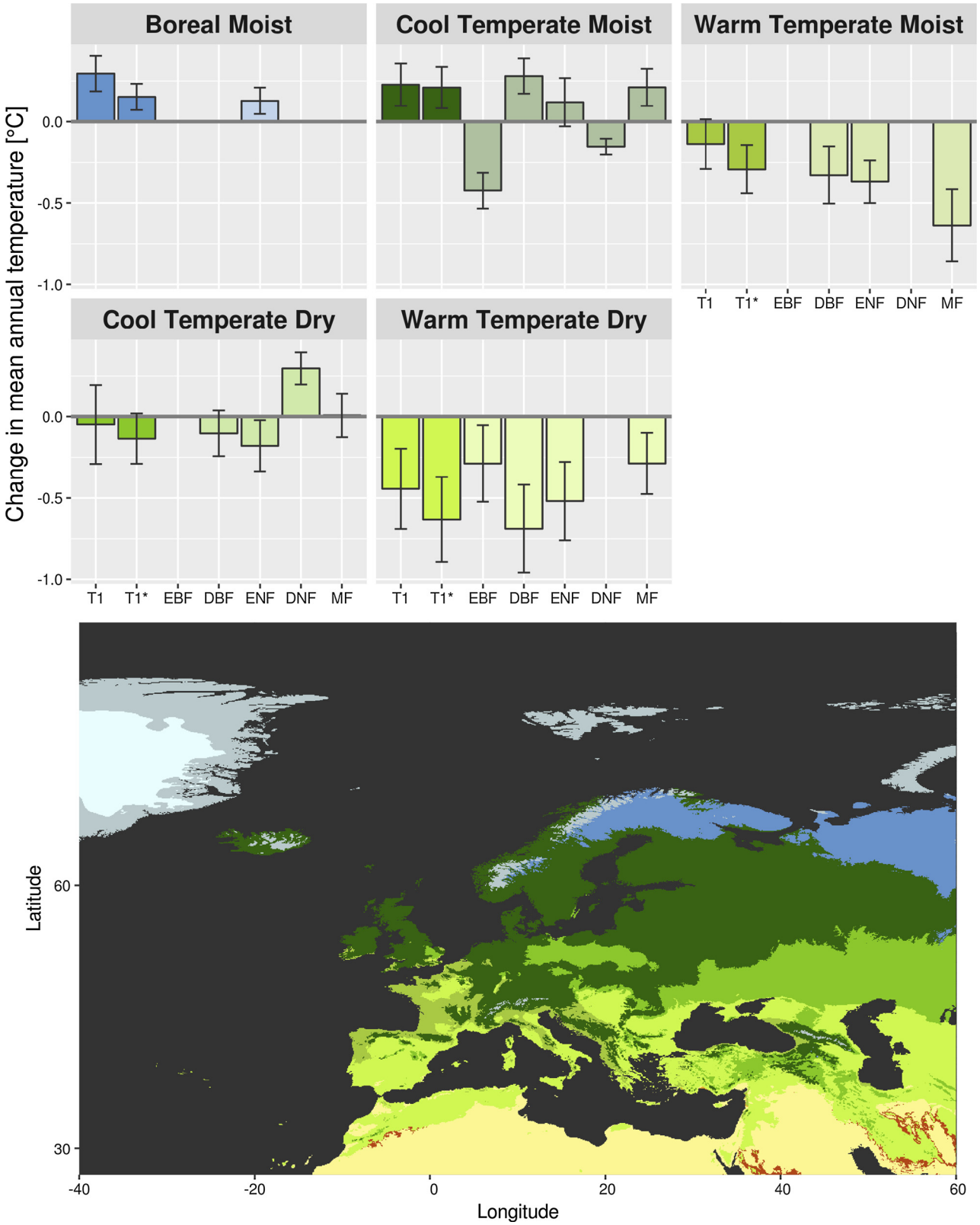

Fig. 4. Illustration of the Tier 2 values for afforestation over the zone comprising Europe and its neighbourhood. The global Tier 1 values per climate zones are reported for reference (labelled T1), along with the Tier 1 generic transition for only this spatial extent (T1*). The Tier 2 transitions, which involve a finer thematic granularity, includes afforestation of cropland towards either evergreen broadleaf forest (EBF), deciduous broadleaf forests (DBF), evergreen needleleaf forests (ENF), deciduous needleleaf forests (DNF) or mixed forests (MF). The map illustrates were the climate zones are located.

under consideration are not included in our estimates, as they are not directly detectable from the observations using the present methodology. As pointed out by recent modelling studies (Winckler et al., 2019), these non-local effects can be important and they should be better understood to ensure that their contribution is not overlooked, especially when larger contiguous patches of land are changed.

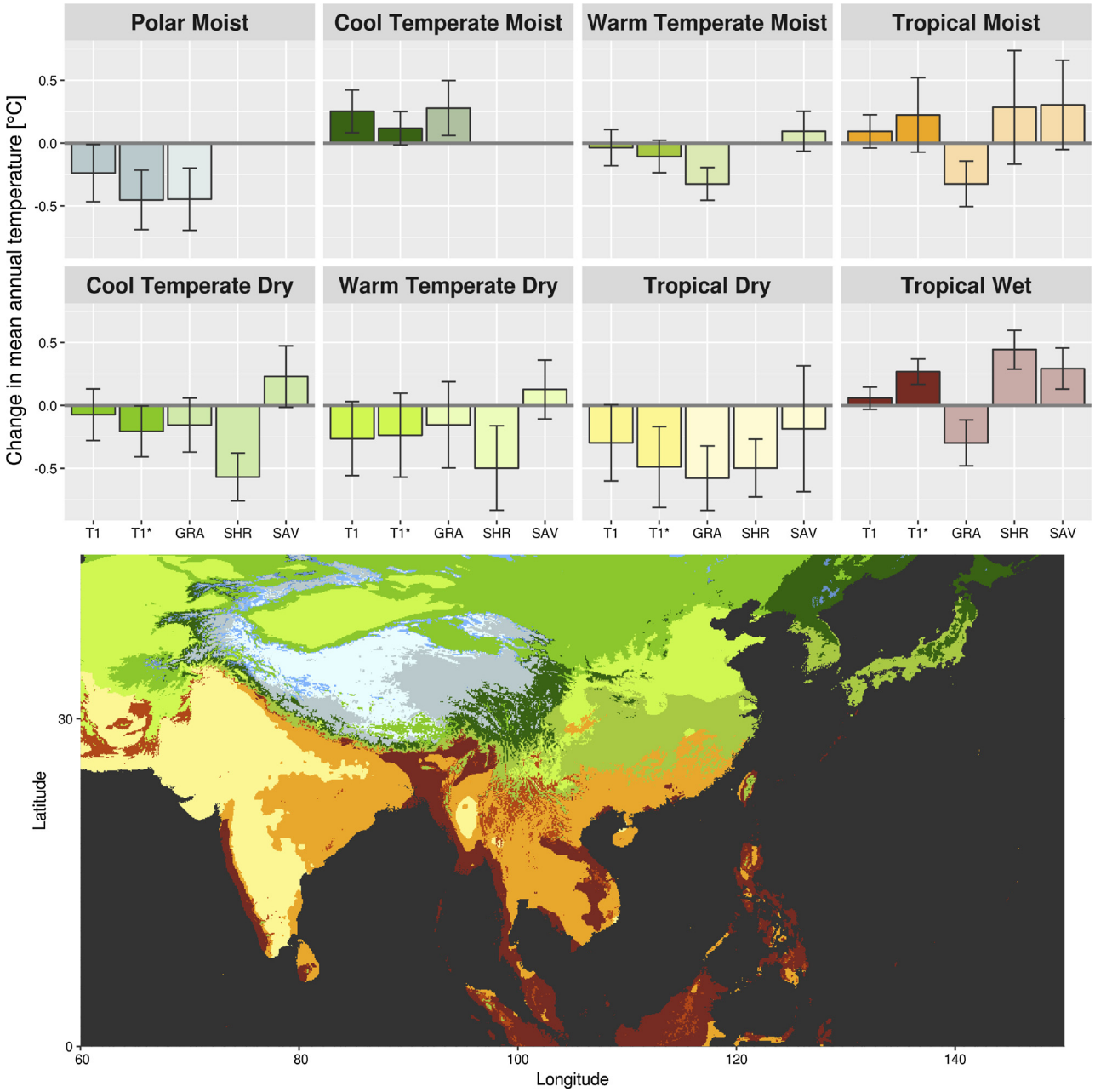

Fig. 5. Illustration of the Tier 2 values for the expansion of croplands into grasslands within the ASIA zone. The global Tier 1 values per climate zones are reported for reference (labelled T1), along with the Tier 1 generic transition for only this spatial extent (T1*). The Tier 2 transitions, which involve a finer thematic granularity, includes the conversion to cropland (CRO) from either grasslands (GRA), shrublands (SHR) or savannas (SAV). The map illustrates were the climate zones are located.

Similarly, the effect of remote LULCC that effectively occur around the world are not integrated either in our estimates. Third, the LULCC considered in this tool are only small in spatial extent, i.e typically smaller than 5 by 5 km^2. This is a necessary consequence from the assumptions of the underlying methodology: when considering a small enough spatial window and correspondingly small changes in LULCC, local direct effects dominate over local indirect effects, and the latter can therefore not affect substantially the hypothesis that neighboring pixels are under similar and thus comparable environmental conditions. Fourth, there is an assumption that land cover did not change substantially during the 2008-2012 period during which satellite observations were used to retrieve the changes in T_{2m}. As land cover is not included in the LST to T_{2m} conversion by Hooker et al. (2018), this may generate larger uncertainty for areas where land cover did occur. Finally, although we provide estimates in terms for LST_{day} and LST_{night} for the sake of completion (for which relevant figures are available in Supplementary Material of this study), we recommend policy-makers to look mainly on the T_{2m} data, which was specifically designed to be more consistent with the near-surface air temperature considered in climate treaties. Furthermore, unlike LST, the data based on T_{2m} has the added value of not suffering from any clear-sky bias since this is integrated in the procedure used to convert LST to T_{2m}.

The present work does not provide a panacea for policy-makers. They cannot presently combine the local BPH effects provided here, which consists of a mean local annual change in T_{2m}, with the BGC effects reported by the IPCC, as these relate to the contribution of a specific land use change to the global CO_2 budget and thus to the mean global annual T_{2m}. Furthermore, the non-local BPH effects are not considered, while the local indirect effects are assumed to be negligible. The solution to include all combined effects would involve fully-

coupled climate models at very fine spatial resolution (e.g. 1 km), but presumably after re-calibrating them with satellite-driven datasets to improve their current shortcomings in estimating local effects (Duveiller et al., 2018a). In the meantime, including the local BPH response represents a substantial improvement over the present situation in which only the BGC response is considered. The spatial dis-aggregation of the information we provide for local BPH effects is also much finer than what policy-makers have currently available for BGC effects. We expect this tool prototype, which takes the current form of the look-up table provided as supplementary material to this paper, will picked up by policy-makers as a first step towards considering the BPH effects of LULCC in a comprehensive assessment of land-based climate policies.

Finally, the effects of LULCC should also be evaluated within a broader scope, both in terms of biophysics, such as its effects on precipitation, but also beyond exclusively climate-centric considerations. Afforestation, for instance, also has large implications for other ecosystem services, such as increasing biodiversity and limiting run-off, which should not be neglected or exchanged for purely BPH reasons. Similarly, the results of Forestland to Cropland/Grassland in the Northern hemisphere showing local cooling should not be interpreted as advocacy for boreal deforestation.

5. Conclusions

The present study presents a proof-of-concept for an assessment tool designed to estimate the potential local biophysical effects of LULCC. The methodological approach enables to reach high quality estimates, while at the same time being applicable worldwide taking into account the criterion of cost-effectiveness in relation to the availability of data and resources. The tool prototype provides a means for comprehensive assessment of LULCC anthropogenic impact on local climate due to radiative and non-radiative LULCC BPH effects. Through the use of this tool, it is possible to assess potential trade-offs or synergies between local and global mitigation, even if the diagnostic for BGC and BPH is not yet fully compatible. For example, afforestation in boreal areas may have a small undesirable BPH warming effect that could be at odds with the mitigation effort of enhancing the carbon sink, even though, at the local level, the warming may be considered beneficial to facilitate food production for example, or reduce hazards to due cold spells in general. Avoiding deforestation in tropical areas is a win-win situation when considering both BPH and BGC processes, as both act towards mitigating of climate warming at both global and local scales. Full understanding of the complete spectrum of short and long term climate consequences of land planning choices is key for an informed and science-based policy making process. While such an endeavour still requires some improvements, such as the incorporation of non-local biophysical effects, the present prototype tool has the potential to directly contribute in the right direction.

Declaration of Interest

The authors declare no competing financial interests.

Acknowledgements

The study was funded by the FP7 LUC4C project (grant no. 603542). All calculations and plots have been realized with R, using the ggplot2, dplyr, sf, ncdf4, raster and randomForest packages.

References

Abdulai, I., Vaast, P., Hoffmann, M.P., Asare, R., Jassogne, L., Van Asten, P., Rötter, R.P., Graefe, S., 2018. Cocoa agroforestry is less resilient to suböoptimal and extreme climate than cocoa in full sun. Global change biology 24 (1), 273–286.

Alkama, R., Cescatti, A., 2016. Biophysical climate impacts of recent changes in global forest cover. Science 351, 600–604. https://doi.org/10.1126/science.aac8083.. URL: http://science.sciencemag.org/content/351/6273/600.abstract.

Anderson-Teixeira, K.J., Snyder, P.K., Twine, T.E., Cuadra, S.V., Costa, M.H., DeLucia, E.H., 2012. Climate-regulation services of natural and agricultural ecoregions of the Americas. Nature Climate Change 2, 177–181 URL: http://www.nature.com/doifinder/10.1038/nclimate1346, 10.1038/nclimate1346.

Betts, R., 2000. Offset of the potential carbon sink from boreal forestation by decreases in surface albedo. Nature 408, 187–190. https://doi.org/10.1038/35041545.

Bonan, G.B., 2008. Forests and climate change: forcings, feedbacks, and the climate benefits of forests. Science 320, 1444–1449. https://doi.org/10.1126/science.1155121.

Breiman, L., 2001. Random Forests. Machine Learning 45, 5–32. https://doi.org/10.1186/1478-7954-9-29.. URL: http://www.springerlink.com/index/U0P06167N6173512.pdf.

Bright, R.M., 2015. Metrics for biogeophysical climate forcings from land use and land cover changes and their inclusion in life cycle assessment: A critical review. Environmental Science and Technology 49, 3291–3303. https://doi.org/10.1021/es505465t.

Bright, R.M., Davin, E., O'Halloran, T., Pongratz, J., Zhao, K., Cescatti, A., 2017. Local temperature response to land cover and management change driven by non-radiative processes. Nature Climate Change 7, 296–302. https://doi.org/10.1038/nclimate3250.. URL: https://www.nature.com/nclimate/journal/v7/n4/full/nclimate3250.html.

Davin, E.L., de Noblet-Ducoudré, N., 2010. Climatic Impact of Global-Scale Deforestation: Radiative versus Nonradiative Processes. Journal of Climate 23, 97–112. https://doi.org/10.1175/2009JCLI3102.1.

Devaraju, N., de Noblet-Ducoudré, N., Quesada, B., Bala, G., 2018. Quantifying the relative importance of direct and indirect biophysical effects of deforestation on surface temperature and teleconnections. Journal of Climate 31, 3811–3829 URL: http://journals.ametsoc.org/doi/10.1175/JCLI-D-17-0563.1, 10.1175/JCLI-D-17-0563.1.

Duveiller, G., Forzieri, G., Robertson, E., Li, W., Georgievski, G., Lawrence, P., Wiltshire, A., Ciais, P., Pongratz, J., Sitch, S., Arneth, A., Cescatti, A., 2018a. Biophysics and vegetation cover change: A process-based evaluation framework for confronting land surface models with satellite observations. Earth System Science Data 10, 1265–1279 URL: https://www.earth-syst-sci-data.net/10/1265/2018/, 10.5194/essd-10-1265-2018.

Duveiller, G., Hooker, J., Cescatti, A., 2018b. A dataset mapping the potential biophysical effects of vegetation cover change. Scientific Data 5, 180014. https://doi.org/10.1038/sdata.2018.14.. URL: https://www.nature.com/articles/sdata201814.

Duveiller, G., Hooker, J., Cescatti, A., 2018c. The mark of vegetation change on Earth's surface energy balance. Nature Communications 9, 679. https://doi.org/10.1038/s41467-017-02810-8.. URL: http://www.nature.com/articles/s41467-017-02810-8.

Ellison, D., Morris, C.E., Locatelli, B., Sheil, D., Cohen, J., Murdiyarso, D., Gutierrez, V., Noordwijk, M.v., Creed, I.F., Pokorny, J., Gaveau, D., Spracklen, D.V., Tobella, A.B., Ilstedt, U., Teuling, A.J., Gebrehiwot, S.G., Sands, D.C., Muys, B., Verbist, B., Springgay, E., Sugandi, Y., Sullivan, C.A., 2017. Trees, forests and water: Cool insights for a hot world. Global Environmental Change 43, 51–61. https://doi.org/10.1016/j.gloenvcha.2017.01.002.. URL: http://linkinghub.elsevier.com/retrieve/pii/S0959378017300134.

ESA, 2017. Land Cover CCI Product User Guide Version 2. Technical Report. . URL: http://maps.elie.ucl.ac.be/CCI/viewer/download/ESACCI-LC-Ph2-PUGv2_2.0.pdf.

Gotangco Castillo, C.K., Raymond, L., Gurney, K.R., 2012. REDD+ and climate: thinking beyond carbon. Carbon Management 3, 457–466.

Grassi, G., House, J., Dentener, F., Federici, S., den Elzen, M., Penman, J., 2017. The key role of forests in meeting climate targets requires science for credible mitigation. Nature Climate Change 7, 220–226 URL: http://www.nature.com/doifinder/10.1038/nclimate3227, 10.1038/nclimate3227.

Grassi, G., Pilli, R., House, J., Federici, S., Kurz, W.A., 2018. Science-based approach for credible accounting of mitigation in managed forests. Carbon Balance and Management 13, 8. https://doi.org/10.1186/s13021-018-0096-2. URL:.

Griscom, B.W., Adams, J., Ellis, P.W., Houghton, R.A., Lomax, G., Miteva, D.A., Schlesinger, W.H., Shoch, D., Siikamäki, J.V., Smith, P., Woodbury, P., Zganjar, C., Blackman, A., Campari, J., Conant, R.T., Delgado, C., Elias, P., Gopalakrishna, T., Hamsik, M.R., Herrero, M., Kiesecker, J., Landis, E., Laestadius, L., Leavitt, S.M., Minnemeyer, S., Polasky, S., Potapov, P., Putz, F.E., Sanderman, J., Silvius, M., Wollenberg, E., Fargione, J., 2017. Natural climate solutions. Proceedings of the National Academy of Sciences 114, 11645–11650 URL: http://www.pnas.org/lookup/doi/10.1073/pnas.1710465114, 10.1073/pnas.1710465114.

Harris, I., Jones, P.D., Osborn, T.J., Lister, D.H., 2014. Updated high-resolution grids of monthly climatic observations - the CRU TS3.10 Dataset. International Journal of Climatology 34, 623–642 URL: http://doi.wiley.com/10.1002/joc.3711, 10.1002/joc.3711.

Ho, T.K., 1998. The random subspace method for constructing decision forests. Pattern Analysis and Machine Intelligence, IEEE... 20, 832–844 URL: http://ieeexplore.ieee.org/xpls/abs_all.jsp?.arnumber=709601 http://cm.bell-labs.com/cm/cs/who/tkh/papers/df.pdf, 10.1109/34.70960.

Hooker, J., Duveiller, G., Cescatti, A., 2018. A global dataset of air temperature derived from satellite remote sensing and weather stations. Scientific Data 5, 180246 URL: http://www.nature.com/articles/sdata2018246, 10.1038/sdata.2018.246.

Houghton, R.A., Nassikas, A.A., 2017. Global and regional fluxes of carbon from land use and land cover change 1850–2015. Global Biogeochemical Cycles 31, 456–472. https://doi.org/10.1002/2016GB005546.

Huang, L., Zhai, J., Liu, J., Sun, C., 2018. The moderating or amplifying biophysical effects of afforestation on CO2-induced cooling depend on the local background climate regimes in China. Agricultural and Forest Meteorology 260-261, 193–203. https://doi.org/10.1016/j.agrformet.2018.05.020. URL:.

IPCC, 2006. 2006 IPCC guidelines for national greenhouse gas inventories. Institute for Global Environmental Strategies, Kanagawa, JP.

Kurz, W.A., Dymond, C.C., White, T.M., Stinson, G., Shaw, C.H., Rampley, G.J., Smyth, C., Simpson, B.N., Neilson, E.T., Trofymow, J.A., Metsaranta, J., Apps, M.J., 2009. CBM-CFS3: A model of carbon-dynamics in forestry and land-use change implementing IPCC standards. Ecological Modelling 220, 480–504 URL: https://www.sciencedirect.com/science/article/pii/S0304380008005012, 10.1016/j.ecolmodel.2008.10.018.

Lawrimore, J.H., Menne, M.J., Gleason, B.E., Williams, C.N., Wuertz, D.B., Vose, R.S., Rennie, J., 2011. An overview of the Global Historical Climatology Network monthly mean temperature data set, version 3. URL: http://doi.wiley.com/10.1029/2011JD016187, 10.1029/2011JD016187.

Le Quéré, C., Andrew, R.M., Friedlingstein, P., Sitch, S., Hauck, J., Pongratz, J., Pickers, P.A., Korsbakken, J.I., Peters, G.P., Canadell, J.G., Arneth, A., Arora, V.K., Barbero, L., Bastos, A., Bopp, L., Chevallier, F., Chini, L.P., Ciais, P., Doney, S.C., Gkritzalis, T., Goll, D.S., Harris, I., Haverd, V., Hoffman, F.M., Hoppema, M., Houghton, R.A., Hurtt, G., Ilyina, T., Jain, A.K., Johannessen, T., Jones, C.D., Kato, E., Keeling, R.F., Goldewijk, K.K., Landschützer, P., Lefèvre, N., Lienert, S., Liu, Z., Lombardozzi, D., Metzl, N., Munro, D.R., Nabel, J.E.M.S., Nakaoka, S.i., Neill, C., Olsen, A., Ono, T., Patra, P., Peregon, A., Peters, W., Peylin, P., Pfeil, B., Pierrot, D., Poulter, B., Rehder, G., Resplandy, L., Robertson, E., Rocher, M., Rödenbeck, C., Schuster, U., Schwinger, J., Séférian, R., Skjelvan, I., Steinhoff, T., Sutton, A., Tans, P.P., Tian, H., Tilbrook, B., Tubiello, F.N., van der Laan-Luijkx, I.T., van der Werf, G.R., Viovy, N., Walker, A.P., Wiltshire, A.J., Wright, R., Zaehle, S., Zheng, B., 2018. Global Carbon Budget 2018. Earth System Science Data 10, 2141–2194 URL: https://www.earth-syst-sci-data.net/10/2141/2018/, 10.5194/essd-10-2141-2018.

Lee, X., Goulden, M.L., Hollinger, D.Y., Barr, A., Black, T.A., Bohrer, G., Bracho, R., Drake, B., Goldstein, A., Gu, L., Katul, G., Kolb, T., Law, B.E., Margolis, H., Meyers, T., Monson, R., Munger, W., Oren, R., Paw, U., Richardson, K.T.A.D., Schmid, H.P., Staebler, R., Wofsy, S., Zhao, L., 2011. Observed increase in local cooling effect of deforestation at higher latitudes. Nature 479, 384–387. https://doi.org/10.1038/nature10588.

Li, Y., Zhao, M., Motesharrei, S., Mu, Q., Kalnay, E., Li, S., 2015. Local cooling and warming effects of forests based on satellite observations. Nature communications 6, 6603. https://doi.org/10.1038/ncomms7603.. URL: http://www.nature.com/ncomms/2015/150325/ncomms7603/full/ncomms7603.html.

Mahmood, R., Pielke, R.a., Hubbard, K.G., Niyogi, D., Dirmeyer, P.a., Mcalpine, C., Carleton, A.M., Hale, R., Gameda, S., Beltrán-Przekurat, A., Baker, B., Mcnider, R., Legates, D.R., Shepherd, M., Du, J., Blanken, P.D., Frauenfeld, O.W., Nair, U.S., Fall, S., 2014. Land cover changes and their biogeophysical effects on climate. International Journal of Climatology 34, 929–953. https://doi.org/10.1002/joc.3736.

Majasalmi, T., Eisner, S., Astrup, R., Fridman, J., Bright, R.M., 2017. An enhanced forest classification scheme for modeling vegetation-climate interactions based on national forest inventory data. Biogeosciences 2017, 1–18. https://doi.org/10.5194/bg-2017-301.. URL: https://www.biogeosciences.net/15/399/2018/ https://www.biogeosciences-discuss.net/bg-2017-301/.

Marland, G., 2003. The climatic impacts of land surface change and carbon management, and the implications for climate-change mitigation policy. Climate Policy 3, 149–157. https://doi.org/10.1016/S1469-3062(03)00028-7.

de Noblet-Ducoudré, N., Boisier, J.P., Pitman, A., Bonan, G.B., Brovkin, V., Cruz, F., Delire, C., Gayler, V., van den Hurk, B.J.J.M., Lawrence, P.J., van der Molen, M.K., Müller, C., Reick, C.H., Strengers, B.J., Voldoire, A., 2012. Determining Robust Impacts of Land-Use-Induced Land Cover Changes on Surface Climate over North America and Eurasia: Results from the First Set of LUCID Experiments. Journal of Climate 25, 3261–3281 URL: http://journals.ametsoc.org/doi/abs/10.1175/JCLI-D-11-00338.1, 10.1175/JCLI-D-11-00338.1.

Peng, S.S., Piao, S., Zeng, Z., Ciais, P., Zhou, L., Li, L.Z.X., Myneni, R.B., Yin, Y., Zeng, H., 2014. Afforestation in China cools local land surface temperature. Proceedings of the National Academy of Sciences of the United States of America. https://doi.org/10.1073/pnas.1315126111.

Perugini, L., Caporaso, L., Marconi, S., Cescatti, A., Quesada, B., De Noblet-Ducoudré, N., House, J.I., Arneth, A., 2017. Biophysical effects on temperature and precipitation due to land cover change. URL: http://stacks.iop.org/1748-9326/12/i=5/a=053002?.key=crossref.c8fcedc7f3570d3a8b7baf3fe79f149c, 10.1088/1748-9326/aa6b3f.

Pesaresi, M., Ehrlich, D., Ferri, S., Florczyk, A.J., Freire, S., Halkia, M., Julea, A., Kemper, T., Soille, P., Syrris, V., 2016. Operating procedure for the production of the Global Human Settlement Layer from Landsat data of the epochs 1975, 1990, 2000, and 2014. https://doi.org/10.2788/253582.

Pielke, R.A., Avissar, R., Raupach, M., Dolman, A.J., Zeng, X., Denning, A.S., et al., 1998. Interactions between the atmosphere and terrestrial ecosystems: influence on weather and climate. Global change biology 4, 461–475.

Pielke, R.a., Marland, G., Betts, R.a., Chase, T.N., Eastman, J.L., Niles, J.O., Niyogi, D.D.S., Running, S.W., 2002. The influence of land-use change and landscape dynamics on the climate system: relevance to climate-change policy beyond the radiative effect of greenhouse gases. Philosophical transactions. Series A, Mathematical, physical, and engineering sciences 360, 1705–1719. https://doi.org/10.1098/rsta.2002.1027.

Pitman, A.J., Avila, F.B., Abramowitz, G., Wang, Y.P., Phipps, S.J., de Noblet-Ducoudré, N., 2011. Importance of background climate in determining impact of land-cover change on regional climate. Nature Climate Change 1, 472–475 URL: http://www.nature.com/doifinder/10.1038/nclimate1294, 10.1038/nclimate1294.

Pitman, A.J., Lorenz, R., 2016. Scale dependence of the simulated impact of Amazonian deforestation on regional climate. Environmental Research Letters 11, 094025 URL: http://stacks.iop.org/1748-9326/11/i=9/a=094025?.key=crossref.46278fc04344cc6f54f1e1f861215bfe, 10.1088/1748-9326/11/9/094025.

Quesada, B., Arneth, A., De Noblet-Ducoudré, N., 2017. Atmospheric, radiative, and hydrologic effects of future land use and land cover changes: A global and multi-model climate picture. Journal of Geophysical Research 122, 5113–5131. https://doi.org/10.1002/2016JD025448.

Ramankutty, N., Foley, J.a., Norman, J., McSweeney, K., 2002. The global distribution of cultivable lands: current patterns and sensitivity to possible climate change. Global Ecology and Biogeography 11, 377–392 URL: http://doi.wiley.com/10.1046/j.1466-822x.2002.00294.x, 10.1046/j.1466-822x.2002.00294.x.

Rockström, J., Gaffney, O., Rogelj, J., Meinshausen, M., Nakicenovic, N., Schellnhuber, H.J., 2017. A Roadmap for Rapid Decarbonization. Science 355, 1269–1271. https://doi.org/10.1126/science.aah3443.

Seneviratne, S.I., Phipps, S.J., Pitman, A.J., Hirsch, A.L., Davin, E.L., Donat, M.G., Hirschi, M., Lenton, A., Wilhelm, M., Kravitz, B., 2018. Land radiative management as contributor to regional-scale climate adaptation and mitigation. Nature Geoscience 11, 88–96. https://doi.org/10.1038/s41561-017-0057-5.

Siebert, S., Döll, P., Hoogeveen, J., Faures, J.M., Frenken, K., Feick, S., 2005. Development and validation of the global map of irrigation areas. Hydrology and Earth System Sciences 9, 535–547 URL: http://www.hydrol-earth-syst-sci.net/9/535/2005/, 10.5194/hess-9-535-2005.

Stocker, B.D., Zscheischler, J., Keenan, T.F., Prentice, I.C., Seneviratne, S.I., Peñuelas, J., 2019. Drought impacts on terrestrial primary production underestimated by satellite monitoring. Nature Geoscience 1URL: http://www.nature.com/articles/s41561-019-0318-6 10.1038/s41561-019-0318-6.

Thiery, W., Davin, E.L., Lawrence, D.M., Hirsch, A.L., Hauser, M., Seneviratne, S.I., 2017. Present-day irrigation mitigates heat extremes. Journal of Geophysical Research: Atmospheres 122, 1403–1422 URL: http://doi.wiley.com/10.1002/2016JD025740, 10.1002/2016JD025740.

UNFCCC, 2011a. Decision 2/CMP.7: Land Use, Land-use Change and Forestry. Publication FCCC/KP/CMP/2011/10/Add.1.

UNFCCC, 2011b. Report of the Conference of the Parties on its sixteenth session, held in Cancun from 29 November to 10 December 2010. Addendum. Part two: Action taken by the Conference of the Parties at its sixteenth session. Technical Report.

United Nations, 2015. Adoption of the Paris Agreement. 21st Conference of the Parties URL: http://unfccc.int/resource/docs/2015/cop21/eng/l09r01.pdf, FCCC/CP/2015/L.9/Rev.1.

West, P.C., Narisma, G.T., Barford, C.C., Kucharik, C.J., Foley, J.a., 2011. An alternative approach for quantifying climate regulation by ecosystems. Frontiers in Ecology and the Environment 9, 126–133. https://doi.org/10.1890/090015.

Winckler, J., Lejeune, Q., Reick, C.H., Pongratz, J., 2019. Nonlocal Effects Dominate the Global Mean Surface Temperature Response to the Biogeophysical Effects of Deforestation. Geophysical Research Letters 46, 745–755 URL: http://doi.wiley.com/10.1029/2018GL080211, 10.1029/2018GL080211.

Winckler, J., Reick, C.H., Luyssaert, S., Cescatti, A., Stoy, P.C., Lejeune, Q., Raddatz, T., Chlond, A., Heidkamp, M., Pongratz, J., 2018. Different response of surface temperature and air temperature to deforestation in climate models. Earth System Dynamics Discussions 1-17URL: https://www.earth-syst-dynam-discuss.net/esd-2018-66/, 10.5194/esd-2018-66.

Winckler, J., Reick, C.H., Pongratz, J., 2017. Robust identification of local biogeophysical effects of land-cover change in a global climate model. Journal of Climate 30, 1159–1176. https://doi.org/10.1175/JCLI-D-16-0067.1.

WMO, 1996a. Guide to Meteorological Instruments and Methods of Observations. WMO report NO.8. 6th edn. pp. 433.

WMO, 1996b. Guide to Meteorological Instruments and Methods of Observations. WMO, Geneva, Switzerland.

Zhang, M., Lee, X., Yu, G., Han, S., Wang, H., Yan, J., Zhang, Y., Li, Y., Ohta, T., Hirano, T., Kim, J., Yoshifuji, N., Wang, W., 2014. Response of surface air temperature to small-scale land clearing across latitudes. Environmental Research Letters 9, 034002 URL: http://stacks.iop.org/1748-9326/9/i=3/a=034002?.key=crossref.efe59fd45fa23ebc584f22a6d2752bca http://iopscience.iop.org/1748-9326/9/3/034002/article/, 10.1088/1748-9326/9/3/034002.

Zhao, C., Liu, B., Piao, S., Wang, X., Lobell, D.B., Huang, Y., Huang, M., Yao, Y., Bassu, S., Ciais, P., Durand, J.L., Elliott, J., Ewert, F., Janssens, I.A., Li, T., Lin, E., Liu, Q., Martre, P., Müller, C., Peng, S., Peñuelas, J., Ruane, A.C., Wallach, D., Wang, T., Wu, D., Liu, Z., Zhu, Y., Zhu, Z., Asseng, S., 2017. Temperature increase reduces global yields of major crops in four independent estimates. Proceedings of the National Academy of Sciences 114, 201701762 URL: http://www.ncbi.nlm.nih.gov/pubmed/28811375 http://www.pubmedcentral.nih.gov/articlerender.fcgi?.artid=PMC5584412 http://www.pnas.org/lookup/doi/10.1073/pnas.1701762114, 10.1073/pnas.1701762114.

Zhao, K., Jackson, R.B., 2014. Biophysical forcings of land-use changes from potential forestry activities in North America. Ecological Monographs 84, 329–353.